Molecular Vision 2024; 30:1-16 <http://www.molvis.org/molvis/v30/1>
Received 17 January 2022 | Accepted 7 February 2024 | Published 10 February 2024

Salidroside ameliorates diabetic retinopathy and Müller cell inflammation via the PI3K/Akt/GSK-3β/NF-kB pathway

Zhen Feng,[1,2] Yang Yang,[1,2] Cai-xing Shi,[3] An-Qi Liu,[1] Chuan-Ling Wu,[4] Wen-Qiang Liu,[1] Sheng-Xue Yu,[1] Hong-Dan Yu,[1] Zhong-Fu Zuo,[1,5] Xue-Zheng Liu[1]

[1]Department of Anatomy, Histology and Embryology, Liaoning Key Laboratory of Diabetic Cognitive and Perceptive Dysfunction, Jinzhou Medical University, Jinzhou, Liaoning, China; [2]Zhejiang Changzheng Vocational Technical College, Shenyang, China; [3]China Medical University, Shenyang, China; [4]Zhejiang Industrial Vocational and Technical College, Shaoxing, Zhejiang, China; [5]Department of Anatomy, Histology and Embryology, Postdoctoral Research Station, Guangxi Medical University, Nanning, Guangxi, China

Purpose: To determine whether salidroside (SAL) modulates inflammatory cytokines in rat retinal Müller cells (rMC-1) in a hyperglycemic environment by investigating the anti-inflammatory mechanisms of SAL in vitro and in vivo.
Methods: A streptozotocin (STZ)-induced diabetic rat model was established to examine the effects of SAL using hematoxylin and eosin (H&E) staining and immunohistochemistry. rMC-1 cells were grown in 50 mM of high-glucose medium. These simulated diabetic conditions were used to evaluate the anti-inflammatory effects of SAL using a Cell Counting Kit-8 (CCK-8) assay, immunofluorescence staining, western blotting, and real-time polymerase chain reaction (qRT–PCR). H&E staining was used to analyze the number of ganglion cells in the retina. rMC-1 lysates were processed for qRT–PCR to measure the steady-state mRNA expression levels of inflammatory markers, such as interleukin 6 (IL-6), interleukin 10 (IL-10), and interleukin 1β (IL-1β). Western blot analysis and immunofluorescence staining were performed to determine the levels of these inflammatory markers.
Results: Our study showed that SAL reversed retinal ganglion cell loss and attenuated nuclear factor kappa B (NF-kB) p65 translocation to the nucleus in STZ-induced diabetic rats. Incubating rMC-1 in different concentrations of SAL for 24 to 48 h affected cell viability. Furthermore, SAL treatment significantly decreased the protein levels of IL-6, TNF-α, and IL-1β compared with those in cells cultured in high glucose (HG). The mRNA expression levels of IL-6 and IL-1β were considerably reduced after SAL treatment, whereas the mRNA expression levels of IL-10 were significantly increased. Interestingly, the beneficial effects of SAL on HG-treated rMC-1 cells were abolished by the PI3K inhibitor LY294002.
Conclusions: These results indicate that SAL treatment reduces cytokine activation in cultured rMC-1. Furthermore, SAL prevents diabetic retinopathy (DR), in part, by modulating the PI3K/Akt/GSK-3β/NF-kB pathway to inhibit Müller cell activation. Thus, SAL is expected to be a potential agent for ameliorating the progression of DR.

Diabetic retinopathy (DR) is a main complication of diabetes and a cause of preventable blindness in adults [1]. Several researchers have shown that chronic inflammation plays a role in the development of DR [2]. In diabetes, the retina produces high levels of proinflammatory cytokines [3,4]. This research suggests that alterations in inflammation play an essential role in the development of DR and that specific cytokines may act as mediators.

Müller cells, which primarily regulate glutamate levels, are the primary glial cells that expand radially to cover nearly the entire width of the retina [5]. These cells are also the principal glial cells in the retina and are thought to be a significant source of inflammatory factors in DR [5-7]. To examine the expression of inflammatory markers in retinal hyperglycemia, we focused on specific inflammatory markers: IL-10, IL-6, tumor necrosis factor-α (TNF-α), IL-1β and nuclear factor-kappa B (NF-kB). Some studies have reported increased levels of cytokines, including IL-1β and IL-6, in the vitreous fluid of patients with proliferative DR and the retinas of diabetic rats [8-10]. The inflammatory response in early diabetes involves cytokine release and activation of critical transcriptional regulatory factors, including NF-kB [11].

Salidroside (SAL) is a bioactive extract from traditional herbal medicines, such as *Robiola rose* [12], which has the functions of preventing tumor growth, delaying aging and reducing oxidative stress [13-17]. Accumulating evidence has demonstrated that SAL exerts favorable anti-inflammatory and antiapoptotic effects [18,19]. In addition, evidence has shown that SAL has a positive impact on multiple complications of diabetes. For example, in the streptozotocin (STZ)-induced neuropathic pain rat model, SAL alleviates pain by inhibiting neuroinflammation in the spinal cord [20].

Correspondence to: Xue-Zheng Liu, Jinzhou Medical University, Department of Anatomy, Histology and Embryology, Jinzhou Medical University, Jinzhou, Liaoning, China 121000, Jinzhou, Liaoning, China: Phone: 13735860792; FAX: 86655; email: 951564552@qq.com

Previous studies have reported that SAL protects retinal endothelial cells from oxidative damage by enhancing the Bcl-2/Bax signaling pathway and activating endogenous antioxidant enzymes [21]. However, no studies have reported whether SAL alleviates the inflammatory response in DR.

Phosphatidylinositol-3-kinase (PI3K) is an essential regulator of multiple signal transduction pathways that mainly controls cell growth, apoptosis, and metabolism [22,23]. The serine/threonine kinase Akt is the downstream target of PI3K and plays a vital role in cell death and survival [24]. A major downstream effector of Akt is glycogen synthase kinase (GSK-3β), which activates the phosphorylation of the serine 9 residue [25]. Studies have shown that mesangial proliferative glomerulonephritis (MPGN) is affected by PI3K/Akt/GSK-3β, inhibiting mesangial cell inflammatory reactions [26]. Activation of the PI3K/Akt/GSK-3β signaling pathway is essential for improving neuroinflammatory responses [27]. Sulforaphene (SF) is one of the main isothiocyanates isolated from Raphani Semen, inhibited the activation of GSK-3β induced by LPS in BV-2 microglia cells and in the STZ-treated rats via increasing the protein expression of the ratio of p-GSK-3β(Ser9). To the best of our knowledge, it remains unclear whether SAL exerts an anti-inflammatory effect on rMC-1 cells by enhancing the PI3K/Akt/GSK-3β pathway.

In the present study, we investigated the anti-inflammatory effect of SAL on DR and explored its underlying mechanisms in vitro. SAL has potential as a treatment for DR, and its anti-inflammatory effect is associated with enhancing the PI3K/Akt/GSK-3β signaling pathway.

METHODS

Animal studies: All experimental procedures were performed according to the National Institutes of Health guidelines and were approved by the Animal Use and Ethics Committee of Jinzhou Medical University. Adult male Sprague Dawley (SD) rats weighing 190–250 g were obtained from the Laboratory Animal Services Centre, Jinzhou Medical University (China, Liaoning). To induce diabetes, eight-week-old SD rats were given intraperitoneal injections of STZ (50 mg/kg, body, Sigma–Aldrich). Blood glucose levels were measured 48 h after STZ injection, and rats with blood glucose levels above 16.7 mmol/l were considered diabetic and selected for research. The rats were randomly assigned to three groups: (1) the control group, (2) the DM group, with type 1 diabetes mellitus [28] (T1DM), and (3) the DM+SAL group, with type 1 diabetes mellitus and SAL treatment. SAL was dissolved in double-distilled water (ddHO) and administered by gavage at a dose of 3 g/kg daily for 12 consecutive weeks.

H&E-staining: To analyze the number of ganglion cells in the retina, the eyes were enucleated, fixed in paraformaldehyde (PFA), and then sliced into 5-µm-thick sections. After being dewaxed in xylene and dehydrated with a graded series of alcohol, the slices were then transferred to hematoxylin for 1–2 min. Next, the sections were placed in an eosin solution for 5–6 min. Finally, images of the slices were taken using a simple microscope. The results were quantified using ImageJ.

Immunohistochemistry: The retinas were removed and fixed with 4% PFA, embedded in paraffin, and cut into 5-µm sections. After xylene dewaxing, the samples were dehydrated with a graded series of alcohol. Next, the antigen was repaired with an epifluorescence microscope (Olympus, Tokyo, Japan), and the sections were blocked in 10% goat serum at room temperature for 30 min. The cells were incubated with anti-p-NF-kB p65 and anti-GS antibodies (mouse, 1:200) at 4 °C overnight. The next day, the specimens were treated with secondary antibodies (1:500, Abcam, anti-mouse, 488-conjugated, fluor647-conjugated anti-rabbit) at room temperature for two hours after being washed with PBS for five min and stained with 4',6-diamidino-2-phenylindole (DAPI; Abcam). Finally, the labeled cells and sections were visualized and processed using an epifluorescence microscope (Olympus, Tokyo, Japan).

Cell viability assay: Cell viability was determined using the Cell Counting Kit-8 assay (Saint-Bion, China) according to the manufacturer's instructions. In brief, cells were cultured in 96-well plates (104 cells/well) in Dulbecco's modified eagle medium (DMEM) and treated with different concentrations of SAL. Subsequently, the cells were analyzed using an automatic microplate reader at 490 nm.

Cell culture and treatment: Cells were purchased from Cell Biolabs (Shanghai, China) and were cultured and passaged in DMEM (HyClone, Logan, UT) containing 10% fetal bovine serum (FBS, Sijiqing, China) with 1% penicillin–streptomycin at 37 °C and 5% CO_2. When the cells reached 70% confluence, they were incubated with high glucose (HG; 50 mM) for 48 h, and some cells were incubated with different concentrations of SAL (50, 100, 200, 400, 500, and 1000 µM) for 24 or 48 h. In addition, cells were pretreated with LY294002 (PI3K blocker) for one h and then incubated with HG and SAL for 48 h. The medium was changed every 24 h to maintain a constant glucose level.

Immunofluorescence analysis: An immunofluorescence analysis was conducted to examine the localization of NF-kB and the expression of cytokines. In brief, rMC-1 cells on coverslips were fixed with 4% paraformaldehyde (PFA) for 30 min. The cells were blocked with a solution containing bovine serum albumin (BSA) and 0.1% Triton X-100 lysis buffer in

PBS, which was followed by incubation at 4 °C with primary antibodies overnight. The primary antibodies were as follows: GS (mouse, Abcam 1:200), NF-kB p-65 (1:1000, CST, Cat# 3033), p-Akt (1:200, Affinity Biosciences, Cat# AF0016), p-GSK-3β (1:500, CST, Cat# 5558), IL-1β (1:200, Bioss, Cat# bs-6319R, China), IL-6 (1:200, Bioss, Cat# bs-6309R, China), and TNF-α (1:200, Immunoway, Cat# YT4689, China). The next day, the cells were treated with secondary antibodies (1:500, Abcam, anti-mouse, 488-conjugated, fluor647-conjugated anti-rabbit) at room temperature for two h after being washed with PBS three times for five min and stained with DAPI (Abcam). The slides were visualized and photographed under a fluorescence microscope (Olympus).

qRT–PCR: Total RNA was extracted using an RNA simple total RNA kit (Tiangen Biotech Co. Ltd, Beijing, China). cDNA was synthesized from 2 μg of total RNA using a PrimeScript RT reagent kit (Invitrogen; Thermo Fisher Scientific, Inc.). PCR was performed using SYBR Premix Ex Taq and specific primers for the target genes, and the results are presented as $2^{-\Delta\Delta ct}$ Table 1.

Western blotting: The cells were collected, washed, and lysed in radioimmunoprecipitation assay (RIPA) buffer. A bicinchoninic acid (BCA) protein assay kit (Solarbio, Beijing, China) was used to measure the protein concentrations of the lysates. Denaturing sample buffer was added to 40–60 μg of protein and loaded onto precast 10% to 12% sodium dodecyl sulfate-PAGE (SDS–PAGE) gels for separation. The protein samples were transferred onto polyvinylidene fluoride (PVDF) membranes and then blocked for two h in 0.5% BSA. The PVDF membranes were incubated overnight at 4 °C with the following antibodies: GAPDH (1:2500, CUSABIO, Cat# CSB-MA000071M0m, China), Akt (1:2000, Affinity, Cat# AF0836), p-Akt (1:2000), GSK-3β (1:2000, CST, Cat# 12,456), p-GSK-3β (1:2000), IL-1β (1:500), IL-6 (1:500), and TNF-α (1:500). The next day, the membranes were washed with tris buffered saline (TBST) three times for five min and incubated with goat-rabbit/mouse IgG (1:5000, Proteintech, Wuhan, China) at room temperature for two h. An electrochemiluminescence (ECL) kit (Solarbio, Beijing, China) was used to observe the immunoreactive bands, and an image analyzer (Bio-Rad) was used for imaging. The relative protein levels were quantified by ImageJ. In addition, ImageJ was used to measure the area and gray value of each band and the gray ratio for each group.

Table 1. The primer sequences.

Gene	Primer (5'-3')
GAPDH	CTACCCACGGCAAGTTCAAC
GAPDH	CCAGTAGACTCCACGACATAC
IL-1β	TCCTCTGTGACTCGTGGGAT
IL-1β	TCAGACAGCACGAGGCATTT
IL-6	CCAGCCAGTTGCCTTCTTG
IL-6	AATTAAGCCTCCGACTTGTGTGAA
IL-10	GTGGAGCAGGTGAAGAATGATT
IL-10	CGTAGGCTTCTATGCAGTTGAT

Statistical analysis: Analysis was performed using GraphPad Prism (version 8.0, GraphPad Software Inc., San Diego, CA). The data are expressed as the mean ± structural equation modeling (SEM). A one-way analysis of variance (ANOVA) with Bonferroni's post hoc test (multiple comparisons) and a *t* test (paired data) were used, and p-values less than 0.05 were considered statistically significant in all tests (Figure 1).

RESULTS

SAL prevented ganglion cell loss due to STZ-induced injury: H&E-stained retinal sections showed a loss of ganglion cells in the diabetic retina compared to the control group. The SAL-treated retinas (3 g/kg bodyweight) showed markedly higher ganglion cell numbers.

SAL altered the distribution of phosphorylated NF-kB p65 in the retinas of STZ-induced diabetic rats: Normally, NF-kB p65 is mainly expressed in the cytoplasm. However, the DR group showed the strongest expression of NF-kB in the outer nuclear layer (ONL) and outer plexiform layer (OPL) compared to the control group. Surprisingly, SAL-treated retinas showed significantly decreased expression of NF-kB p65 in the ONL. As shown in Figure 2, these results indicate the nuclear translocation of NF-kB p65, but SAL treatment reduced the intranuclear expression of NF-kB p65.

Immunocytochemical characterization of cultured rMC-1 cells: The identities of the cultured rMC-1 cells were confirmed by immunocytochemistry using antibodies against the rMC-1 marker GS. Nuclei were stained with DAPI. Almost all cells were positive for GS (Figure 3).

SAL had no cytotoxic effects on rMC-1 viability: To investigate the effect of SAL on the viability of rMC-1 cells, CCK-8 assays were performed. As shown in Figure 4A,B, the number of viable rMC-1 cells was not significantly different compared to the control group. This result indicates that SAL (0–1000 μM) had no cytotoxic effects on rMC-1 cells.

SAL reduced the HG-induced expression of proinflammatory cytokines and suppressed the nuclear translocation of NF-kB p65 in rMC-1 cells: IL-1β and IL-6 are important inflammatory cytokine markers. As shown in Figure 5, there were significantly increased protein levels of IL-1β, IL-6, and TNF-α when rMC-1 cells were under HG conditions

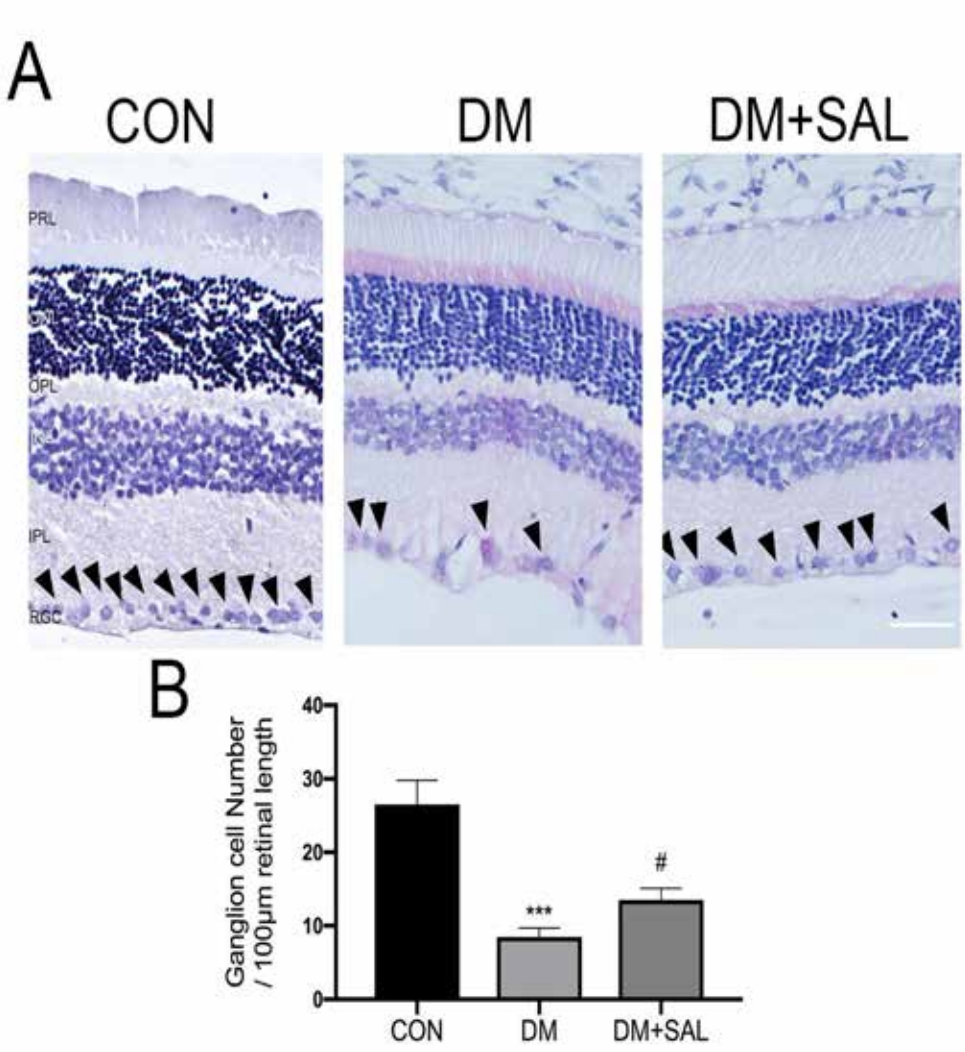

Figure 1. SAL prevents ganglion cell loss due to STZ-induced injury. **A**: H&E staining showing that SAL protects ganglion cells in diabetic rats. The arrowheads represent retinal ganglion cells. **B**: Quantitative analysis of the number of ganglion cells. SAL-treated retinas showed a significantly higher number of ganglion cells than the DM group. ($^{\#}p<0.05$). Values are presented as mean ± SD (n=3). Scale bar=100 μm. ***p<0.001, versus CON group. $^{\#}p<0.05$, versus DM group.

compared to the cells treated with different concentrations of SAL. In addition, in rMC-1 cells treated with different concentrations of SAL (100 μM, 200 μM, 500 μM), the expression of proinflammatory cytokines was significantly inhibited in a dose-dependent manner. Thus, we chose 500 μM as our experimental concentration. To determine cellular localization, each treatment (CON, HG, HG+SAL) was performed in triplicate, and 15 images were captured per well using a fluorescence microscope. Figure 6 shows that pretreatment with SAL significantly reduced the nuclear translocation of NF-kB p65 compared with that in the HG group.

SAL influenced the PI3K/Akt/GSK-3β signaling pathway under HG conditions: To further demonstrate the role of the PI3K/Akt/GSK-3β signaling pathway in the anti-inflammatory effects of SAL, rMC-1 cells were preincubated with 500 μM SAL for six h and then treated with or without 50 mmol/L glucose for 48 h. The phosphorylation of Akt and GSK-3β was detected by western blotting and immunofluorescence analysis. SAL had a protective effect, potentially by activating the PI3K/Akt/GSK-3β signaling pathway. As shown in Figure 7 and Figure 8, the protein levels of p-Akt and P-GSK-3β were markedly decreased in rMC-1 cells that were treated with HG, whereas treatment with SAL caused a marked increase in p-Akt and p-GSK-3β levels compared

with those in the HG groups. To further explore the effect of SAL on this pathway, rMC-1 cells were pretreated with LY294002 (20 μM). The levels of p-Akt and p-GSK-3β/GSK-3β were significantly decreased. These results demonstrate that treatment with SAL enhances the activation of p-Akt and p-GSK-3β.

SAL influenced the mRNA expression of inflammatory factors in rMC-1 cells: HG can induce an inflammatory response in rMC-1 cells. To clarify the anti-inflammatory effects of SAL on rMC-1 cells, the mRNA expression levels of IL-6, IL-1β, and IL-10 were determined by q-PCR. As shown in Figure 9A-C, SAL significantly upregulated the level of IL-10 mRNA induced by HG and reduced the mRNA expression levels of IL-6 and IL-1β. However, LY294002 increased the mRNA expression of inflammatory factors and reduced the anti-inflammatory effect of SAL. These results indicate that SAL inhibits the HG-mediated inflammatory response in rMC-1 cells through the Akt/GSK-3β signaling pathway.

SAL reduced the HG-induced expression of proinflammatory cytokines in rMC-1 cells through the PI3K/Akt/GSK-3β signaling pathway: To explore SAL-mediated effects on PI3K/Akt/GSK-3β in rMC-1, 20 μM of LY204002 was incubated with rMC-1 cells. As shown in Figure 10 and Figure 11, the expression levels of the inflammation-associated proteins IL-1β, IL-6, and TNF-α were detected by western blotting and immunofluorescence analysis. Compared to the control

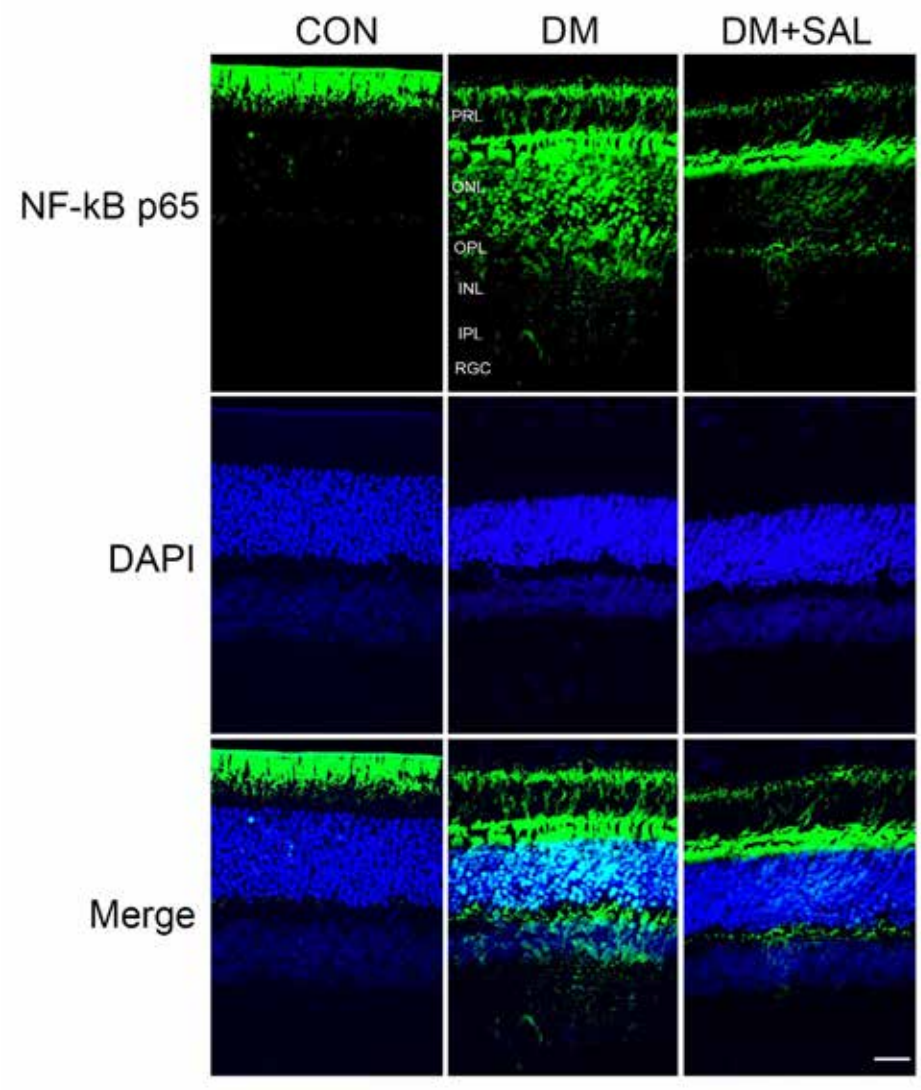

Figure 2. SAL affects the distribution of phosphorylated NF-kB p65 in the retinas of STZ-induced diabetic rats. Detection of the distribution of NF-kB p65 in the retina by immunofluorescence analysis. NF-kB p65 is mainly expressed in the cytoplasm. The DM group showed increased expression in the ONL and INL. SAL-treated mice showed relatively lower expression in the ONL and INL.

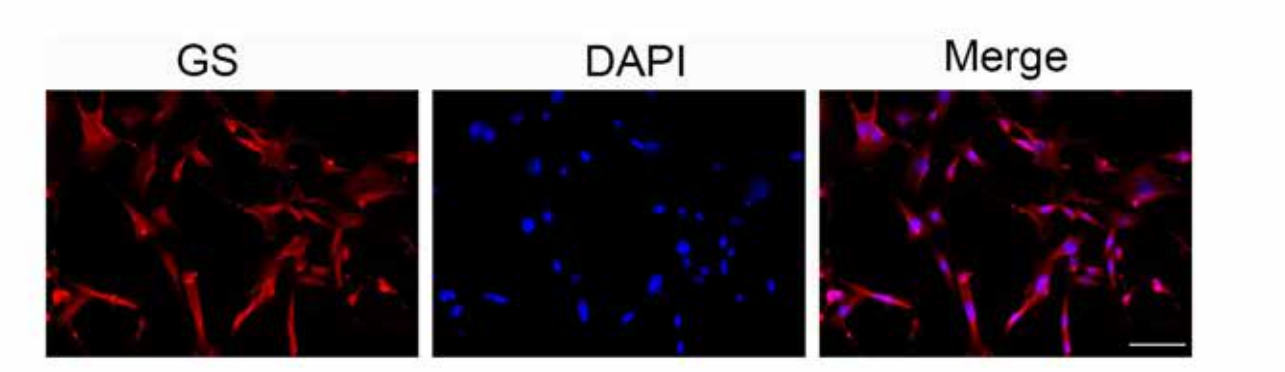

Figure 3. Immunocytochemical analysis of rMC-1 cell cultures. Red: rMC-1 stained for GS. Blue: nuclear staining with DAPI. Merged labeling of GS. Scale bar=100 µm.

group, HG markedly increased the protein expression of IL-1β, IL-6, and TNF-α. SAL treatment reduced the expression levels of inflammation-related proteins compared to the HG group. Treatment with LY294002 significantly increased the protein expression of IL-1β, IL-6, and TNF-α compared to the SAL-treated group and decreased the anti-inflammatory effect of SAL. These results show that suppression of the PI3K/Akt/GSK-3β signaling pathway attenuated the anti-inflammatory effect of SAL.

SAL attenuated the phosphorylation of NF-kB p65 and its nuclear translocation by enhancing the PI3K/Akt/GSK-3β signaling pathway: As shown in Figure 12, NF-kB p65 was markedly translocated to the nucleus after HG treatment compared to the control group. However, rMC-1 cells treated with SAL exhibited decreased NF-kB p65 translocation to the nucleus compared to cells treated with HG. However, LY294002 promoted NF-kB p65 translocation to the nucleus. These results suggest that treatment with SAL can reduce NF-kB p65 translocation to the nucleus induced by HG through the activation of PI3K/Akt/GSK/3β.

DISCUSSION

SAL is a common traditional Chinese medicine (TCM) that has been widely used to enhance tumor growth and protect the cardiovascular system [29]. The favorable effects of SAL on various chronic diseases have been described previously. Moreover, emerging evidence has indicated that SAL has great therapeutic potential for treating diabetic encephalopathy [12,30], and it has been shown to effectively inhibit oxidative stress through the Akt/GSK-3β/NrF2 pathway in an ischemia/reperfusion SD rat model [31]. Studies have also shown that SAL improves lower limb motor function and neuronal tissue damage in rats with spinal cord injuries by reducing the gene expression and production of IL-1β, IL-6, and TNF-α [32]. As previously described, Müller cells are the

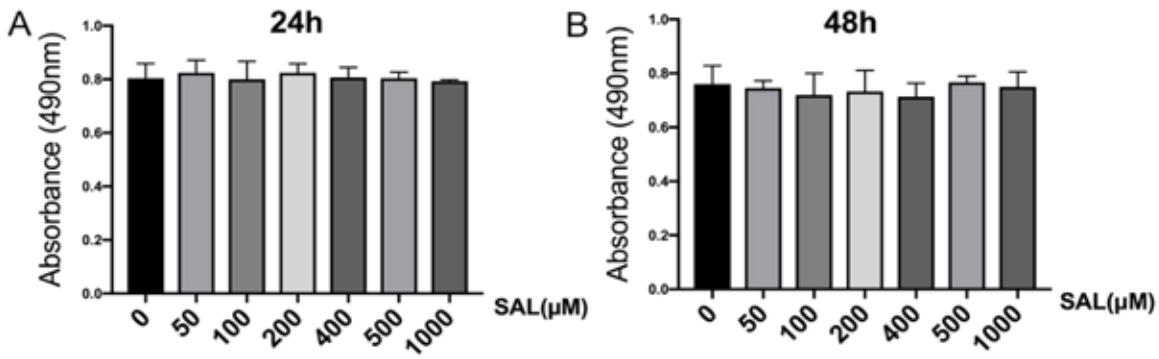

Figure 4. SAL had no cytotoxic effects on rMC-1 viability, as measured using the CCK-8 kit. **A**: rMC-1 cells were incubated with increasing concentrations of SAL for 24 h at 37 °C. **B**: rMC-1 cells were incubated with increasing concentrations of SAL for 48 h at 37 °C. There was no significant reduction in viable cell numbers after treatment with SAL at concentrations up to 1000 µM.

principal glial cell type in the retina [5] and are essential for maintaining normal retinal function.

To the best of our knowledge, no evidence has yet been presented to suggest that SAL has anti-inflammatory effects in vivo or in vitro through the PI3K/Akt/GSK-3β signaling pathway. Therefore, we studied the anti-inflammatory effects of SAL on rMC-1 cells under HG conditions using an STZ-induced diabetes rat model.

Previous studies have reported that DR promotes apoptosis in retinal ganglion cells and decreases retinal thickness and GS expression [33,34]. In the present study, we observed the protective effects of SAL against DR and explored the underlying mechanism. We used in vitro and in vivo systems to determine the following:

1. In vivo, we first verified the anti-inflammatory and protective effects of salidroside against STZ-induced DR. Compared with the control group, the DR group of rats exhibited significantly increased nuclear translocation of NF-kB p65 and the loss of ganglion cells. However, these effects were ameliorated by SAL treatment.

2. In vitro, we observed that salidroside suppressed the release of IL-1β, IL-6, and TNF-α and inhibited NF-kB p65 nuclear translocation by enhancing the PI3K/Akt/GSK-3β signaling pathway induced by HG. These results indicate that PI3K/Akt/GSK-3β might be the anti-inflammatory signaling pathway mediated by SAL in DR. Our findings strongly suggest that SAL may possess protective anti-inflammatory potential in DR.

Inflammation plays an important role in the development of DR, and Müller cells are major factors in the secretion of inflammatory factors [2,35]. Generally, NF-kB p65 is located within the cytoplasm and is kept inactive by interactions with

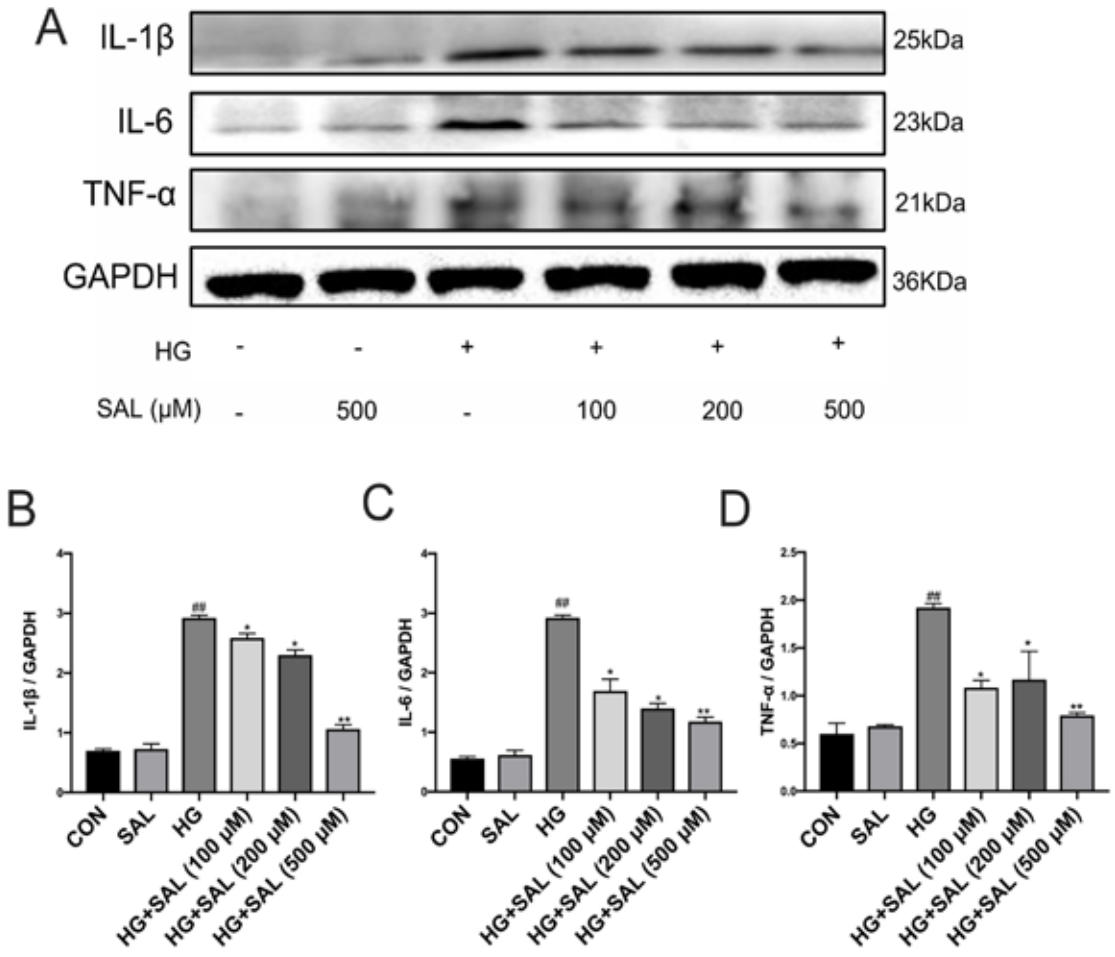

Figure 5. SAL reduced the HG-induced expression of proinflammatory cytokines. rMC-1 cells were pretreated with different concentrations of SAL (100, 200, 500 μM) for 6 h and then stimulated with HG (50 mM) for 48 h. **A**: The levels of IL-1β, IL-6, and TNF-α were determined by western blotting. **B**–**D**: Quantitative analyses of the protein expression of IL-1β, IL-6, and TNF-α.

its inhibitor. Once activated, phosphorylated NF-kB dimers are released and translocate to the nucleus, which induces the production of cytokines [36-38]. A prior study reported that NF-kB p65 nuclear localization occurs in Müller cells exposed to LPS [39]. In our study, we demonstrated that NF-kB p65 significantly translocated to the nucleus in DR. Furthermore, we determined whether SAL induced the expression of IL-1β, IL-6, and TNF-α under HG conditions in rMC-1 cells. After these cytokines were detected by western blotting and immunofluorescence, the results showed that the expression of IL-1β, IL-6, and TNF-α was increased, but SAL treatment reduced the expression of cytokines and NF-kB p65 translocation to the nucleus. These results indicate that Müller cell secretion of cytokines is affected by SAL-mediated anti-inflammatory effects under HG conditions.

The Akt/GSK-3β signaling pathway plays a pivotal role in neuroinflammation and neuroprotection [40]. The inactivation of GSK-3β, which is mainly regulated through the phosphorylation of Ser-9 (p-GSK-3β), participates in the inhibition of inflammatory reactions and pain [41,42]. Therefore,

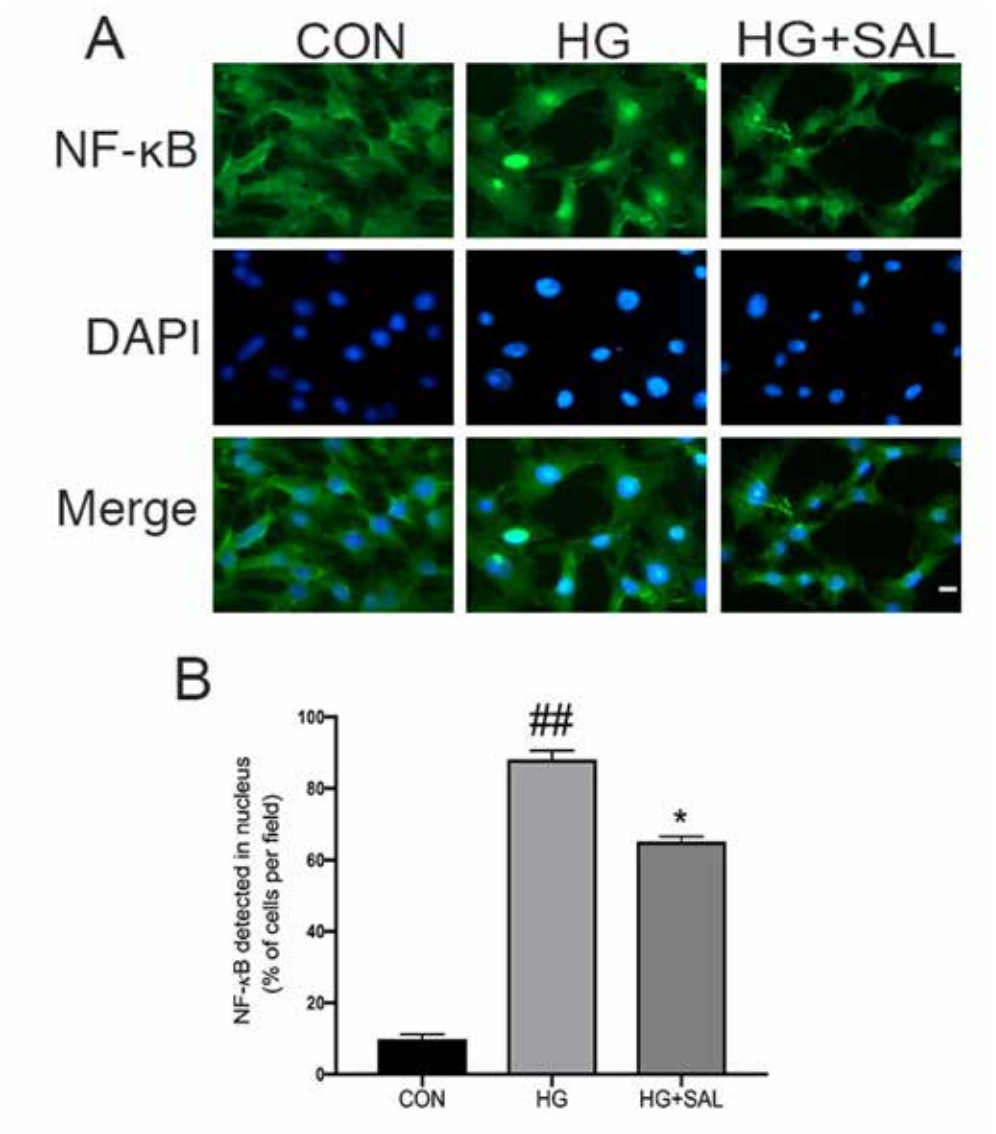

Figure 6. SAL suppresses the nuclear translocation of NF-kB p65 in rMC-1 cells. **A**: The nuclear translocation of NF-kB p65 was determined using microscopy. **B**: Fifteen fields were imaged per well, and cells showing nuclear translocation of NF-kB were counted. These data are expressed as a ratio to the total number of cells in the field. The experiments were performed in triplicate, and the values are expressed as the percentage of cells per field that localized NF-kB to the nucleus. Scale bar=50 µm. *p<0.05, **p<0.01, ***p<0.001, versus CON group. ##p<0.01, versus HG group.

we examined the PI3K/Akt/GSK-3β signaling pathway to elucidate the mechanisms through which SAL modulates the inflammatory response and attenuates NF-kB p65 translocation to the nucleus in rMC-1 cells. Our data indicated that SAL preconditioning significantly enhanced the phosphorylation of Akt and GSK-3β at Ser-9.

Although our findings demonstrate the importance of the anti-inflammatory effects of SAL on DR, there are some caveats and limitations that need to be addressed in future studies. We focused on the anti-inflammatory effect of SAL on rMC-1 cells. However, inflammation is regulated by multiple types of retinal cells in addition to rMC-1 cells, such as microglial and vascular endothelial cells [43,44]. Previous studies have reported that the injury responses of activated Müller cells and microglial cells in the retina are not independent but rather involve bidirectional feedback signals [45]. Therefore, in future experiments, the study of Müller–microglial coculture systems would be useful to further examine the anti-inflammatory role of SAL in DR. Taken together, these data demonstrate that SAL alleviates rMC-1 cell inflammation induced by HG through the activation of PI3K/Akt/GSK-3β signaling. Moreover, PI3K/Akt/

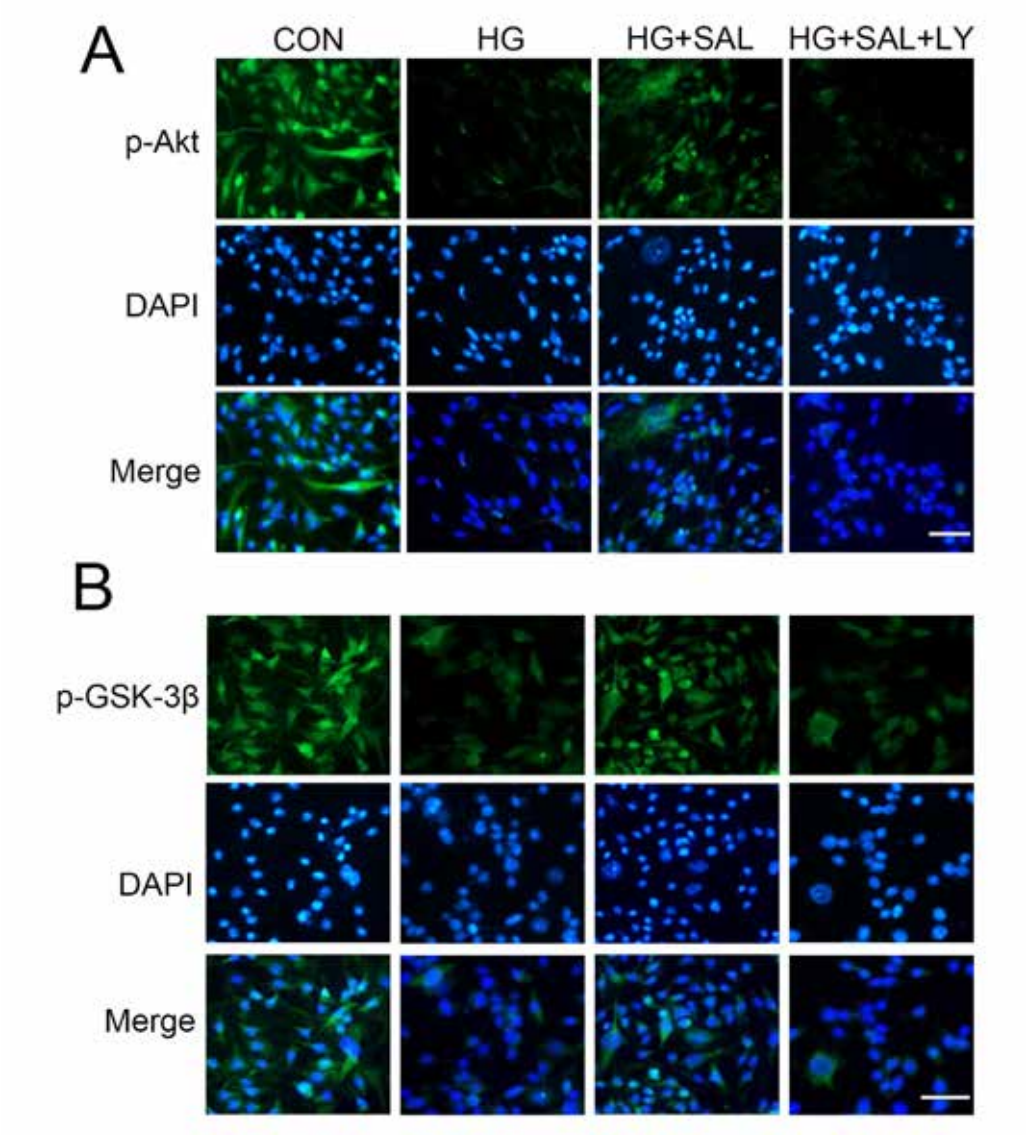

Figure 7. SAL influenced the PI3K/Akt/GSK-3β signaling pathway under HG conditions. **A**: western blot analyses were used to determine the protein expression of p-Akt and p-GSK-3β. The protein levels of p-Akt and P-GSK-3β were markedly decreased in rMC-1 cells treated with HG, whereas treatment with SAL caused a marked increase in p-Akt and p-GSK-3β compared with that in the HG groups. **B**–**C**: Quantitative results of protein density determination. *p<0.05, versus CON group. #p<0.05, versus HG group. □p<0.05, versus HG+SAL group.

GSK-3β phosphorylation was associated with NF-kB translocation to the nucleus and HG-induced rMC-1 cell secretion of cytokines.

In conclusion, our study demonstrates that SAL treatment attenuates HG-induced inflammation in rMC-1 cells by activating the PI3K/Akt/GSK-3β signaling pathway. The findings provide additional evidence supporting the clinical use of SAL for its anti-inflammatory effect and to protect retinal function in DR. However, further experiments are needed to elucidate the intrinsic mechanism of SAL.

Acknowledgments

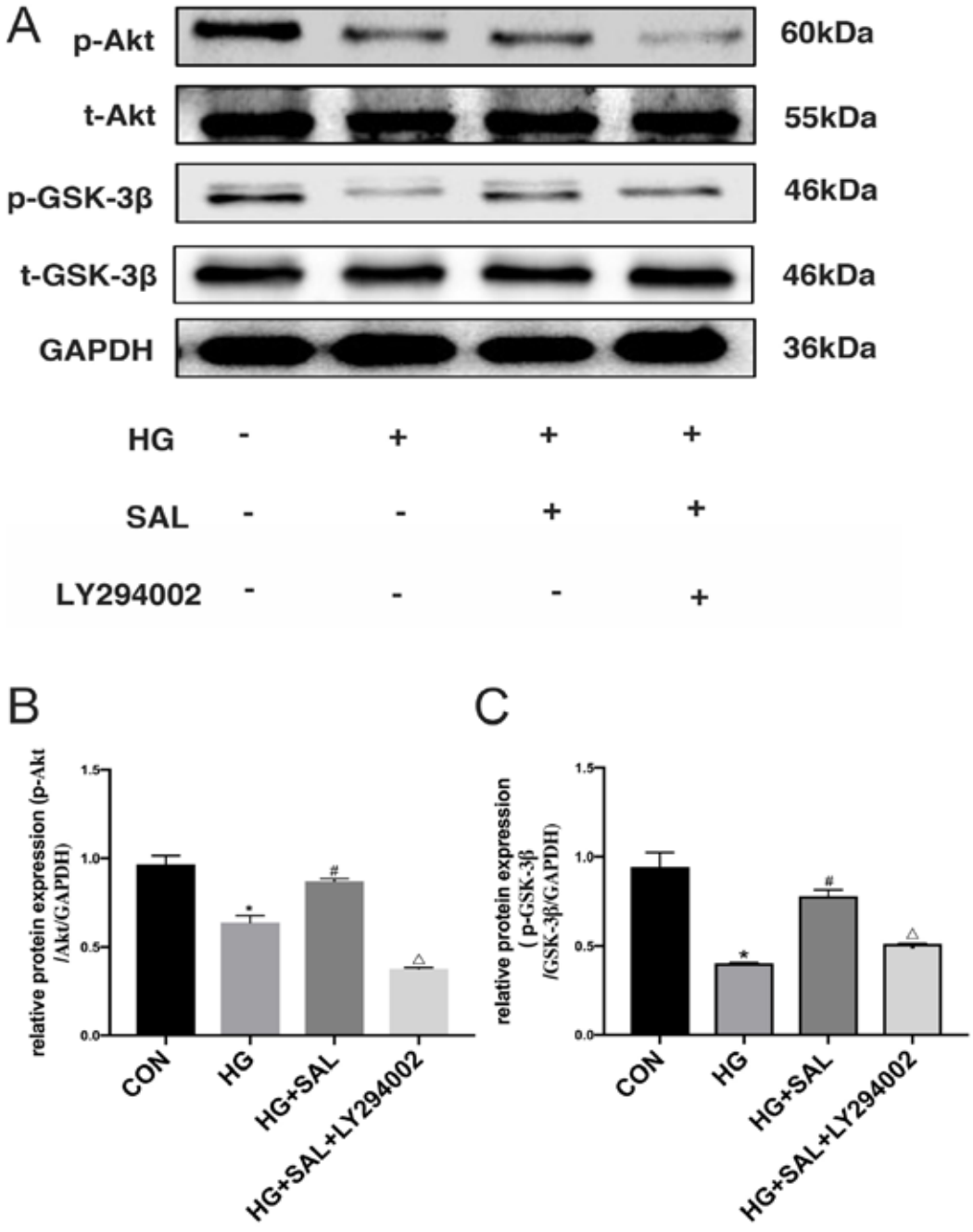

Figure 8. SAL influenced the PI3K/Akt/GSK-3β signaling pathway under HG conditions. Immunofluorescence detection of the protein expression p-Akt and p-GSK-3β. The results were consistent with the western blot results. Values are presented as mean ± SD (n=3). Scale bar=100 μm.

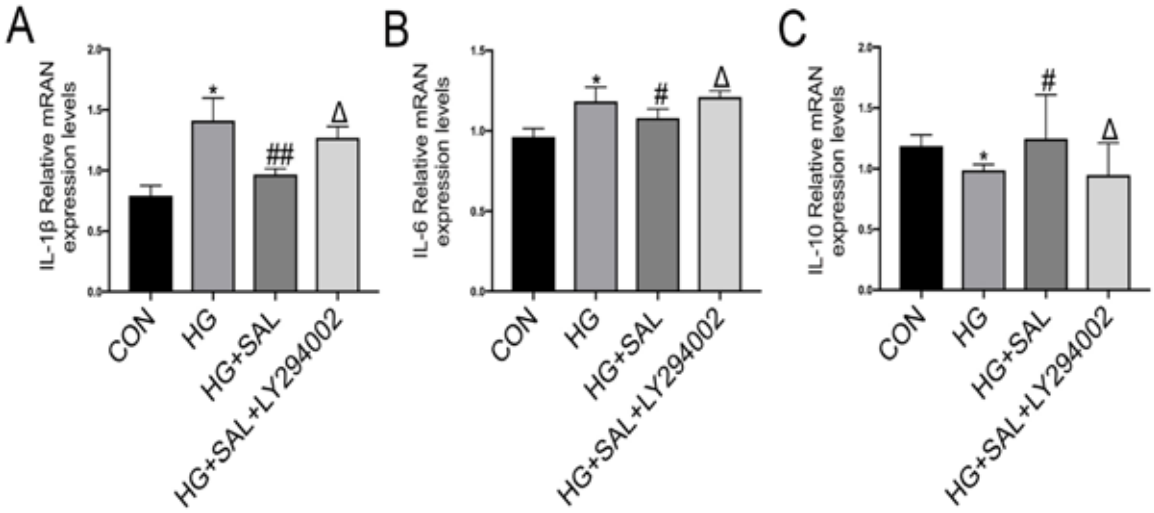

Figure 9. SAL influenced the mRNA expression of inflammatory factors in rMC-1 cells. The mRNA expression of IL-1β, IL-6, and IL-10 was determined by qRT–PCR. **A**–**B**: The mRNA levels of IL-1β and IL-6 were significantly decreased in rMC-1 cells cultured with SAL compared with those in the HG group ($^{\#\#}p<0.01$). **C**: The mRNA expression levels of IL-10. In the SAL group, the mRNA levels of IL-10 were significantly increased compared with those in the HG group. Values are presented as mean ± SD (n=3). *p<0.05, versus CON group. $^{\#}p<0.05$, $^{\#\#}p<0.01$, versus HG+SAL group. $^{\Delta}p<0.05$, versus HG+SAL group.

Authors' contributions: XZL and ZFZ designed the experiments. YY and CXS conducted the experiments and animal study. ZF analyzed the experiment data and prepared all figures. AQL, CLW, WQL, SXY and HDY provided technical support. ZF wrote the manuscript. Declaration of conflicting interests The author(s) declared no potential conflicts of interest with respect to the, research, authorship, and publication of this article. Funding The author(s) disclosed receipt of the following financial support for the research, authorship, and publication of this article: This work was supported by the Foundation of Education Department of Liaoning Province (N0s. LJKMZ20221241). Dr. Xue-Zheng Liu (951564552@qq.com) and Dr. Zhong-Fu Zuo (164352674@qq.com) are co-corresponding authors for this paper.

REFERENCES

1. Tang J, Kern TS. Inflammation in diabetic retinopathy. Prog Retin Eye Res 2011; 30:343-58. [PMID: 21635964].

2. Joussen AM, Poulaki V, Le ML, Koizumi K, Esser C, Janicki H, Schraermeyer U, Kociok N, Fauser S, Kirchhof B, Kern TS, Adamis AP. A central role for inflammation in the pathogenesis of diabetic retinopathy. FASEB J 2004; 18:1450-2. [PMID: 15231732].

3. Goldberg RB. Cytokine and cytokine-like inflammation markers, endothelial dysfunction, and imbalanced coagulation in development of diabetes and its complications. J Clin Endocrinol Metab 2009; 94:3171-82. [PMID: 19509100].

4. Semeraro F, Cancarini A, dell'Omo R, Rezzola S, Romano MR, Costagliola C. Diabetic Retinopathy: Vascular and Inflammatory Disease. J Diabetes Res 2015; 2015:582060[PMID: 26137497].

5. Newman E, Reichenbach A. The Müller cell: a functional element of the retina. Trends Neurosci 1996; 19:307-12. [PMID: 8843598].

6. Tsacopoulos M, Magistretti PJ. Metabolic coupling between glia and neurons. J Neurosci 1996; 16:877-85. [PMID: 8558256].

7. Mizutani M, Gerhardinger C, Lorenzi M. Müller cell changes in human diabetic retinopathy. Diabetes 1998; 47:445-9. [PMID: 9519752].

8. Abu el Asrar AM, Maimone D, Morse PH, Gregory S, Reder AT. Cytokines in the vitreous of patients with proliferative diabetic retinopathy. Am J Ophthalmol 1992; 114:731-6. [PMID: 1463043].

9. Carmo A, Cunha-Vaz JG, Carvalho AP, Lopes MC. L-arginine transport in retinas from streptozotocin diabetic rats: correlation with the level of IL-1 beta and NO synthase activity. Vision Res 1999; 39:3817-23. [PMID: 10748917].

10. Yuuki T, Kanda T, Kimura Y, Kotajima N, Tamura J, Kobayashi I, Kishi S. Inflammatory cytokines in vitreous fluid and serum of patients with diabetic vitreoretinopathy. J Diabetes Complications 2001; 15:257-9. [PMID: 11522500].

11. Busik JV, Mohr S, Grant MB. Hyperglycemia-induced reactive oxygen species toxicity to endothelial cells is dependent on paracrine mediators. Diabetes 2008; 57:1952-65. [PMID: 18420487].

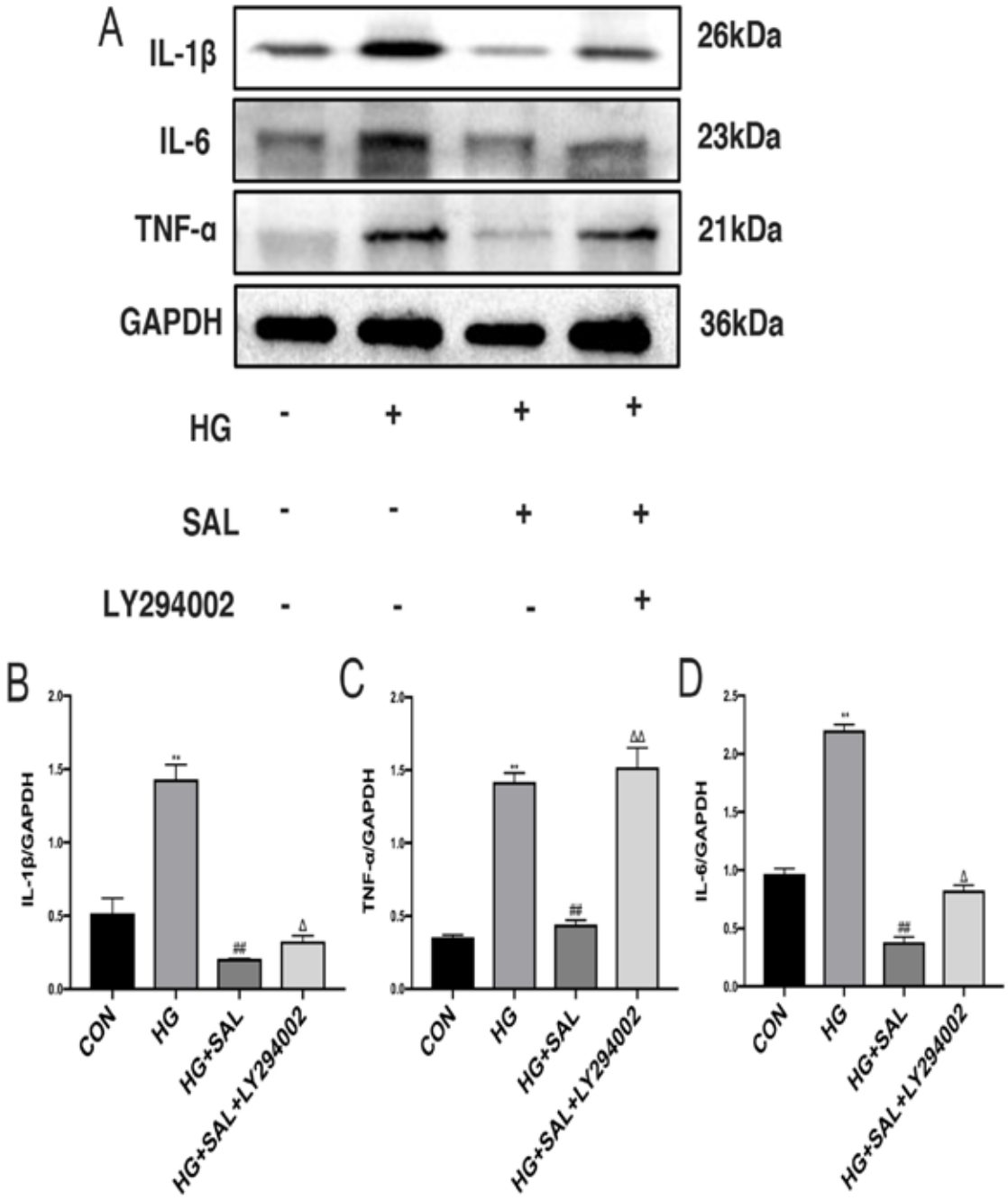

Figure 10. SAL reduced the HG-induced expression of pro-inflammatory cytokines in rMC-1 through the PI3K/Akt/GSK-3β signaling pathway. Western blot analysis of cytokine expression. **A–D**: western blot analysis of protein expression and quantitative analyses of IL-1β, IL-6, and TNF-α. **p<0.01, versus CON group. #p<0.05, ##p<0.01, versus HG group. △p<0.05, △△p<0.01 versus HG+SAL group.

12. Lee SY, Lai FY, Shi LS, Chou YC, Yen IC, Chang TC. Rhodiola crenulata extract suppresses hepatic gluconeogenesis via activation of the AMPK pathway. Phytomedicine 2015; 22:477-86. [PMID: 25925970].

13. Li X, Sipple J, Pang Q, Du W. Salidroside stimulates DNA repair enzyme Parp-1 activity in mouse HSC maintenance. Blood 2012; 119:4162-73. [PMID: 22427203].

14. Tang H, Gao L, Mao J, He H, Liu J, Cai X, Lin H, Wu T. Salidroside protects against bleomycin-induced pulmonary

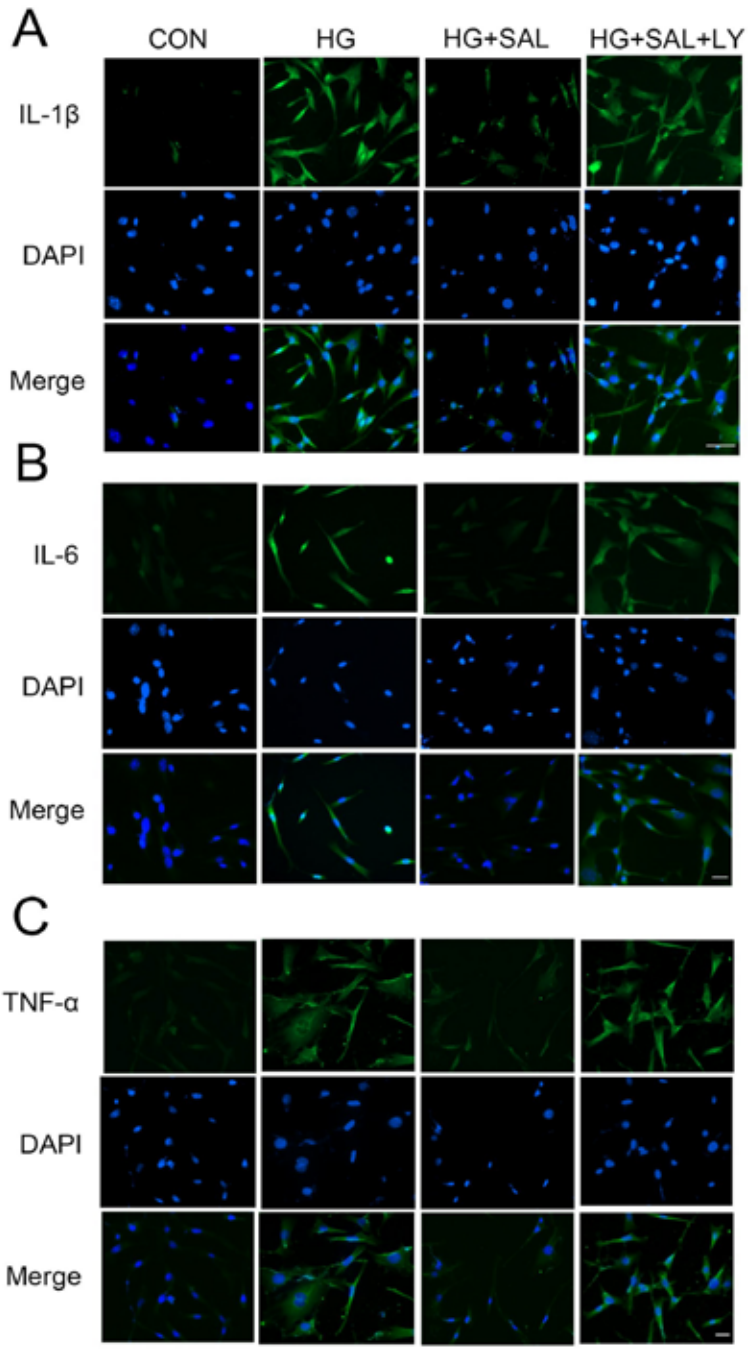

Figure 11. SAL reduced the HG-induced expression of pro-inflammatory cytokines in rMC-1 through the PI3K/Akt/GSK-3β signaling pathway. The protein expression of IL-1β, IL-6, and TNF-α was determined by immunofluorescence analysis. The results were consistent with the western blot results. Values are presented as mean ± SD (n=3). Scale bar=100 μm.

fibrosis: activation of Nrf2-antioxidant signaling, and inhibition of NF-κB and TGF-β1/Smad-2/-3 pathways. Cell Stress Chaperones 2016; 21:239-49. [PMID: 26577463].

15. Wang M, Luo L, Yao L, Wang C, Jiang K, Liu X, Xu M, Shen N, Guo S, Sun C, Yang Y. Salidroside improves glucose homeostasis in obese mice by repressing inflammation in white adipose tissues and improving leptin sensitivity in hypothalamus. Sci Rep 2016; 6:25399-[PMID: 27145908].

16. Zhang J, Zhen YF, Pu-Bu-Ci-Ren , Song LG, Kong WN, Shao TM, Li X, Chai XQ. Salidroside attenuates beta amyloid-induced cognitive deficits via modulating oxidative stress and inflammatory mediators in rat hippocampus. Behav Brain Res 2013; 244:70-81. [PMID: 23396166].

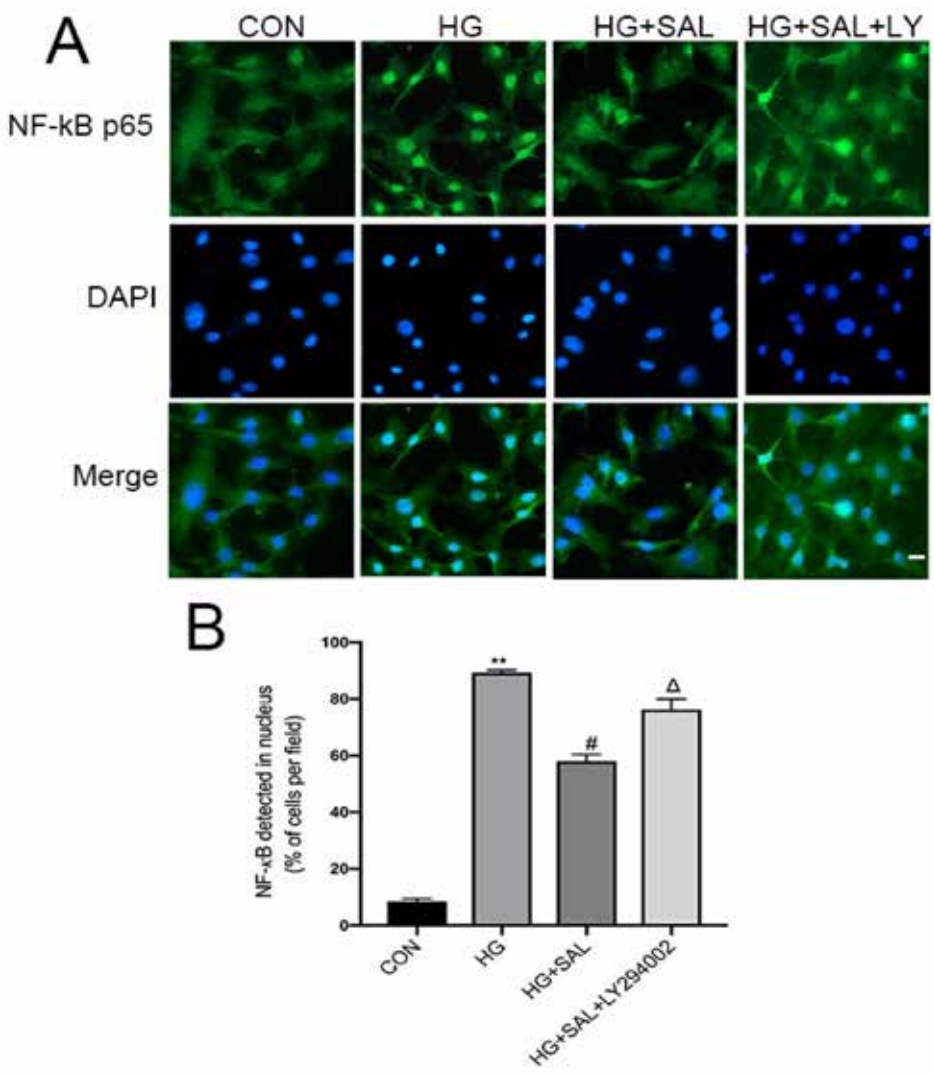

Figure 12. SAL attenuated phosphorylation of NF-kB p65 translocation to the nucleus by enhancing the PI3K/Akt/GSK-3β signaling pathway. Immunofluorescence analysis of NF-kB p65 translocation to the nucleus in rMC-1 cells. **A**: The nuclear translocation of NF-kB p65 was determined by microscopy. **B**: Fifteen fields were imaged per well, and cells in which NF-kB was located in the nucleus were counted. These data are expressed as a ratio to the total number of cells in the field. The experiments were performed in triplicate, and the values are expressed as the percentage of cells per field that localized NF-kB to the nucleus. Values are presented as mean ± SD (n=3). Scale bar=50 μm. **p<0.01, versus CON group. #p<0.05, versus HG group. Δp<0.05, versus HG+SAL group.

17. Zhao G, Shi A, Fan Z, Du Y. Salidroside inhibits the growth of human breast cancer in vitro and in vivo. Oncol Rep 2015; 33:2553-60. [PMID: 25814002].

18. Hu H, Li Z, Zhu X, Lin R, Chen L. Salidroside Reduces Cell Mobility via NF- κ B and MAPK Signaling in LPS-Induced BV2 Microglial Cells. Evid Based Complement Alternat Med 2014; 2014:383821[PMID: 24864151].

19. Liu X, Wen S, Yan F, Liu K, Liu L, Wang L, Zhao S, Ji X. Salidroside provides neuroprotection by modulating microglial polarization after cerebral ischemia. J Neuroinflammation 2018; 15:39-[PMID: 29426336].

20. Ni GL, Cui R, Shao AM, Wu ZM. Salidroside Ameliorates Diabetic Neuropathic Pain in Rats by Inhibiting Neuroinflammation. J Mol Neurosci 2017; 63:9-16. [PMID: 28741143].

21. Shi K, Wang X, Zhu J, Cao G, Zhang K, Su Z. Salidroside protects retinal endothelial cells against hydrogen peroxide-induced injury via modulating oxidative status and apoptosis.

Biosci Biotechnol Biochem 2015; 79:1406-13. [PMID: 25921655].

22. Fruman DA, Chiu H, Hopkins BD, Bagrodia S, Cantley LC, Abraham RT. The PI3K Pathway in Human Disease. Cell 2017; 170:605-35. [PMID: 28802037].

23. Zhang H, Li F, Pan Z, Wu Z, Wang Y, Cui Y. Activation of PI3K/Akt pathway limits JNK-mediated apoptosis during EV71 infection. Virus Res 2014; 192:74-84. [PMID: 25116390].

24. Li C, Zhang J, Ma Z, Zhang F, Yu W. miR-19b serves as a prognostic biomarker of breast cancer and promotes tumor progression through PI3K/AKT signaling pathway. Onco Targets Ther 2018; 11:4087-95. [PMID: 30038508].

25. Wang CD, Yuan CF, Bu YQ, Wu XM, Wan JY, Zhang L, Hu N, Liu XJ, Zu Y, Liu GL, Song FZ. Fangchinoline inhibits cell proliferation via Akt/GSK-3beta/ cyclin D1 signaling and induces apoptosis in MDA-MB-231 breast cancer cells. Asian Pac J Cancer Prev 2014; 15:769-73. [PMID: 24568493].

26. Liu B, Lin J, Bai L, Zhou Y, Lu R, Zhang P, Chen D, Li H, Song J, Liu X, Wu Y, Wu J, Liang C, Zhou J. Paeoniflorin Inhibits Mesangial Cell Proliferation and Inflammatory Response in Rats With Mesangial Proliferative Glomerulonephritis Through PI3K/AKT/GSK-3β Pathway. Front Pharmacol 2019; 10:978-[PMID: 31551783].

27. Yang W, Liu Y, Xu QQ, Xian YF, Lin ZX. Sulforaphene Ameliorates Neuroinflammation and Hyperphosphorylated Tau Protein via Regulating the PI3K/Akt/GSK-3*β* Pathway in Experimental Models of Alzheimer's Disease. Oxid Med Cell Longev 2020; 2020:4754195[PMID: 32963694].

28. King AJ. The use of animal models in diabetes research. Br J Pharmacol 2012; 166:877-94. [PMID: 22352879].

29. Sun L, Dou F, Chen J, Chi H, Xing S, Liu T, Sun S, Chen C. Salidroside slows the progression of EA.hy926 cell senescence by regulating the cell cycle in an atherosclerosis model. Mol Med Rep 2018; 17:257-63. [PMID: 29115447].

30. Ma YG, Wang JW, Zhang YB, Wang BF, Dai ZJ, Xie MJ, Kang HF. Salidroside improved cerebrovascular vasodilation in streptozotocin-induced diabetic rats through restoring the function of BK_{Ca} channel in smooth muscle cells. Cell Tissue Res 2017; 370:365-77. [PMID: 28803422].

31. Cai L, Li Y, Zhang Q, Sun H, Yan X, Hua T, Zhu Q, Xu H, Fu H. Salidroside protects rat liver against ischemia/reperfusion injury by regulating the GSK-3β/Nrf2-dependent antioxidant response and mitochondrial permeability transition. Eur J Pharmacol 2017; 806:32-42. [PMID: 28411054].

32. Su Y, Zong S, Wei C, Song F, Feng H, Qin A, Lian Z, Fu F, Shao S, Fang F, Wu T, Xu J, Liu Q, Zhao J. Salidroside promotes rat spinal cord injury recovery by inhibiting inflammatory cytokine expression and NF-κB and MAPK signaling pathways. J Cell Physiol 2019; 234:14259-69. [PMID: 30656690].

33. Kumar B, Gupta SK, Nag TC, Srivastava S, Saxena R, Jha KA, Srinivasan BP. Retinal neuroprotective effects of quercetin in streptozotocin-induced diabetic rats. Exp Eye Res 2014; 125:193-202. [PMID: 24952278].

34. Zeng K, Yang N, Wang D, Li S, Ming J, Wang J, Yu X, Song Y, Zhou X, Yang Y. Resveratrol Prevents Retinal Dysfunction by Regulating Glutamate Transporters, Glutamine Synthetase Expression and Activity in Diabetic Retina. Resveratrol Prevents Retinal Dysfunction by Regulating Glutamate Transporters, Glutamine Synthetase Expression and Activity in Diabetic Retina. Neurochem Res 2016; 41:1050-64. [PMID: 26677078].

35. Gerhardinger C, Costa MB, Coulombe MC, Toth I, Hoehn T, Grosu P. Expression of acute-phase response proteins in retinal Müller cells in diabetes. Invest Ophthalmol Vis Sci 2005; 46:349-57. [PMID: 15623795].

36. Bhat NR, Feinstein DL, Shen Q, Bhat AN. p38 MAPK-mediated transcriptional activation of inducible nitric-oxide synthase in glial cells. Roles of nuclear factors, nuclear factor kappa B, cAMP response element-binding protein, CCAAT/enhancer-binding protein-beta, and activating transcription factor-2. J Biol Chem 2002; 277:29584-92. [PMID: 12048217].

37. Jana M, Dasgupta S, Liu X, Pahan K. Regulation of tumor necrosis factor-alpha expression by CD40 ligation in BV-2 microglial cells. J Neurochem 2002; 80:197-206. [PMID: 11796758].

38. Nakajima K, Matsushita Y, Tohyama Y, Kohsaka S, Kurihara T. Differential suppression of endotoxin-inducible inflammatory cytokines by nuclear factor kappa B (NFkappaB) inhibitor in rat microglia. Neurosci Lett 2006; 401:199-202. [PMID: 16580131].

39. Shanmugam A, Wang J, Markand S, Perry RL, Tawfik A, Zorrilla E, Ganapathy V, Smith SB. Sigma receptor 1 activation attenuates release of inflammatory cytokines MIP1γ, MIP2, MIP3α, and IL12 (p40/p70) by retinal Müller glial cells. J Neurochem 2015; 132:546-58. [PMID: 25439327].

40. Golpich M, Amini E, Hemmati F, Ibrahim NM, Rahmani B, Mohamed Z, Raymond AA, Dargahi L, Ghasemi R, Ahmadiani A. Glycogen synthase kinase-3 beta (GSK-3β) signaling: Implications for Parkinson's disease. Pharmacol Res 2015; 97:16-26. [PMID: 25829335].

41. Gao M, Yan X, Weng HR. Inhibition of glycogen synthase kinase 3β activity with lithium prevents and attenuates paclitaxel-induced neuropathic pain. Neuroscience 2013; 254:301-11. [PMID: 24070631].

42. Martins DF, Rosa AO, Gadotti VM, Mazzardo-Martins L, Nascimento FP, Egea J, López MG, Santos AR. The antinociceptive effects of AR-A014418, a selective inhibitor of glycogen synthase kinase-3 beta, in mice. J Pain 2011; 12:315-22. [PMID: 20705523].

43. Han J, Li Y, Liu X, Zhou T, Sun H, Edwards P, Gao H, Yu FS, Qiao X. Metformin suppresses retinal angiogenesis and inflammation in vitro and in vivo. PLoS One 2018; 13:e0193031[PMID: 29513760].

44. Yuan Z, Chen X, Yang W, Lou B, Ye N, Liu Y. The anti-inflammatory effect of minocycline on endotoxin-induced

uveitis and retinal inflammation in rats. Mol Vis 2019; 25:359-72. [PMID: 31354229].

45. Wang M, Ma W, Zhao L, Fariss RN, Wong WT. Adaptive Müller cell responses to microglial activation mediate neuroprotection and coordinate inflammation in the retina. J Neuroinflammation 2011; 8:173-[PMID: 22152278].

Articles are provided courtesy of Emory University and the Zhongshan Ophthalmic Center, Sun Yat-sen University, P.R. China. The print version of this article was created on 10 February 2024. This reflects all typographical corrections and errata to the article through that date. Details of any changes may be found in the online version of the article.